of protein synthesis occurs in heavy polyribosomes, whereas most of the newly synthesized cytoplasmic mRNA is found in structures separate from these, in the light polyribosomes and in RNP particles. The name "informosome" has been proposed (*2*) for these RNP particles, since they are believed to bear genetic information or mRNA. That these RNP particles are separate entities and not simply complexes of mRNA with ribosomal fragments might be concluded from the evidence of their buoyant density (*2*, *3*).

If any new mRNA does not participate in protein synthesis (*6–9*), we should expect that a means for regulating its activity is available in the cytoplasm. The existence of such mRNA-protein complexes as informosomes would allow us to formulate at least two hypothetical ways in which the activity of mRNA could be programmed, or protein synthesis regulated before or during translation: (i) The fate of particular messenger RNA's might hinge on that of the informosomes to which they belong. This fate may be investigated from the standpoint of the metabolic stability of the RNA or its ability to form polyribosomes through interaction with ribosomes. Such an interaction has been indicated already (*2*) in the fish embryo. (ii) Another method for regulation is offered if the mRNA remains complexed with protein during polyribosome formation. Such a sustained complex might allow the protein of the informosome to exert an influence on template function. Consistent with the idea of such an inactive polyribosome would be the interpretation of Figs. 2 and 3*a*, that the light polyribosomes containing newly synthesized messenger RNA are for the most part not engaged in protein synthesis. That they are incompletely loaded with ribosomes is indicated by their range of sedimentation constants and the range of sizes of their mRNA deducible from sedimentation behavior (*4*).

A solely cytoplasmic regulation of protein synthesis appears to be operative immediately after fertilization (*6–9*). Such a regulation may certainly influence embryogenesis and cellular differentiation.

ALEXANDER S. SPIRIN*
MARTIN NEMER
Institute for Cancer Research, Fox Chase, Philadelphia 11, Pennsylvania

References and Notes

1. N. V. Belitsina, M. A. Ajtkhozhin, L. P. Gavrilova, A. S. Spirin, *Biokhimiya* **29**, 363 (1964).
2. A. S. Spirin, N. V. Belitsina, M. A. Ajtkhozhin, *Zh. Obstch. Biol.* **25**, 321 (1964).
3. A. S. Spirin, N. V. Belitsina, M. A. Ajtkhozhin, L. P. Ovtchinnikov, in preparation.
4. M. Nemer and A. A. Infante, *Science*, this issue.
5. M. Nemer, *Proc. Natl. Acad. Sci. U.S.* **50**, 230 (1963); F. Wilt, *Biochem. Biophys. Res. Commun.* **11**, 447 (1963).
6. E. B. Harvey, *Biol. Bull.* **71**, 101 (1936); **79**, 166 (1940).
7. P. C. Denny and A. Tyler, *Biochem. Biophys. Res. Commun.* **14**, 245 (1964).
8. A. A. Neyfakh, *Zh. Obstch. Biol.* **20**, 202 (1959).
9. P. R. Gross and G. H. Cousineau, *Biochem. Biophys. Res. Commun.* **10**, 321 (1963); P. R. Gross, L. I. Malkin, W. A. Moyer, *Proc. Natl. Acad. Sci. U.S.* **51**, 407 (1964).
10. M. Nemer and S. G. Bard, *Science* **140**, 664 (1963).
11. M. Nemer and A. A. Infante, in preparation.
12. D. W. Stafford, W. H. Sofer, R. M. Iverson, *Proc. Natl. Acad. Sci. U.S.* **52**, 313 (1964).
13. A. Monroy and A. Tyler, *Arch. Biochem. Biophys.* **103**, 431 (1963).
14. Supported by grants CA 05936-04 and CA 06927-03 from the National Institutes of Health.
* Permanent address: Bakh Institute of Biochemistry, Academy of Sciences of U.S.S.R., Moscow.

29 March 1965

Messenger RNA in Early Sea-Urchin Embryos: Size Classes

Abstract. *Rapidly labeled RNA from four-cell embryos and blastulae of sea urchins was analyzed by sedimentation and for ability to form DNA-RNA hybrids. The RNA was derived from polyribosomes and from the "gel interphase," an extraction compartment resulting from treatment of whole embryos with phenol and known to be enriched with nuclei. The RNA from both sources displayed a high degree of structural complementarity to DNA. This DNA-like RNA of the polyribosomes sedimented in discrete classes, rather than in the sedimentation continuum demonstrable for the labeled RNA of the gel interphase. Thus messenger RNA appears to emerge in the cytoplasm in discrete size classes.*

The information for embryonic development resides ultimately in the messenger RNA's (*1*) which direct the synthesis of specific proteins. We have attempted to characterize, particularly through sedimentation analysis, the messenger RNA (mRNA) synthesized by early sea-urchin embryos. We now describe the peculiarities of the rapidly labeled RNA derived both from its nuclear site of origin and from its ultimate site of functionality in protein synthesis, the polyribosome (*2*).

In higher organisms rapidly labeled RNA is located predominantly in the nucleus of the cell (*3*). However, only a portion of the nuclear RNA may be messenger, as judged by the criteria of being either DNA-like (D-RNA) (*4*, *5*) or being able to stimulate incorporation into protein (*6*). In the rapidly growing cells usually studied a large proportion of the labeled nuclear RNA is precursor to ribosomal RNA (*7*, *8*). However, in the early embryo of the sea urchin *Lytechinus pictus*, the labeled RNA from a cellular partition that may be equivalent to the nucleus is predominantly D-RNA. The relative proportion of D-RNA in this compartment decreases with development of the embryo.

Labeled RNA that can be considered predominantly messenger, according to its DNA-like base composition, has been extracted from polyribosomes of tissue culture cells and analyzed by ultracentrifugation (*9*). The rapidly labeled RNA derived from polyribosomes (*9*, *10*) and that of total or nuclear pulse-labeled RNA (*4*, *7*, *11*, *12*) both display a polydisperse continuum upon sedimentation. Such patterns support the concept that mRNA synthesized by the cell consists of hundreds of molecular species in a continuous array of sizes; this array would account for the spectrum of known sizes of proteins. In our study with homogenates from early embryos we have uncovered a situation in which mRNA, derived from polyribosomes, appears to have been produced in discrete size classes.

All of the rapidly synthesized RNA of the cell can be obtained through extraction with 0.5 percent sodium dodecyl sulfate (SDS) and phenol at 60°C (*11*). All the pulse-labeled RNA was extracted by this procedure from embryos at the 4-hour cleavage stage, which had been incubated with uridine-H^3 for 15 minutes, and from 10-hour blastulae, incubated for 10 minutes. The purified RNA (*13*) was then submitted to sedimentation analysis. The sedimentation diagram (Fig. 1) indicated a polydisperse continuum throughout the gradient with a peak at approximately 10*S*. The labeled RNA of the blastula was also polydisperse,

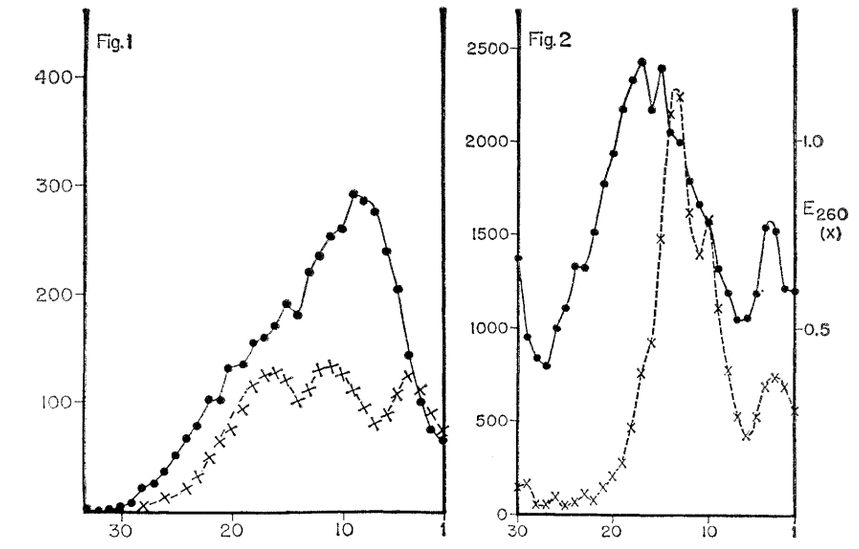

Fig. 1. Sedimentation diagram of pulse-labeled RNA from cleavage-stage embryo. Four-hour embryos (16- to 32-cell stage, 1 ml) were incubated in 5 ml of sea water with 7.5 μM uridine-H^3 (4 c/mmole) for 15 minutes at 19°C, and then frozen at −80°C. Embryos were homogenized in six volumes of acetate buffer (*13*) containing SDS and then shaken with an equal volume of phenol at 60°C. The extracted RNA was further purified (*13*) and then centrifuged through 5 to 20 percent (weight/volume) sucrose gradients in the Spinco rotor SW 39 at 38,000 rev/min for 3 hours. P^{32}-labeled ribosomal and 4*S* RNA were included as marker (**X**). Fractions were assayed directly (*17*).

Fig. 2. Sedimentation diagram of pulse-labeled RNA from blastulae. Ten-hour blastulae were incubated for 10 minutes with 5 μM uridine and treated exactly as in Fig. 1. After sedimentation, optical densities (E_{260}) were measured, and radioactivity was assayed as in Fig. 1.

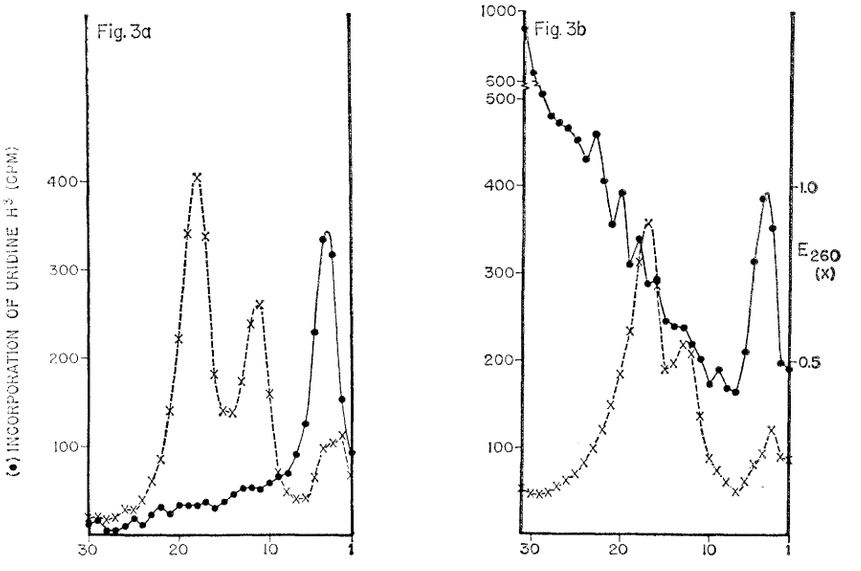

Fig. 3. Sedimentation diagrams of differentially extracted pulse-labeled RNA from blastulae of *L. pictus*. Twelve-hour blastulae (1 ml per 5 ml of sea water) were incubated as in Fig. 2. (*a*) The embryos were homogenized in six volumes of acetate buffer (*13*) without SDS, then shaken with an equal volume of phenol at 20°C. (*b*) The embryos were treated as in Fig. 2. RNA samples were centrifuged through 5 to 20 percent (weight/volume) sucrose gradients for 10 hours in the Spinco SW 25.1 rotor at 25,000 rev/min.

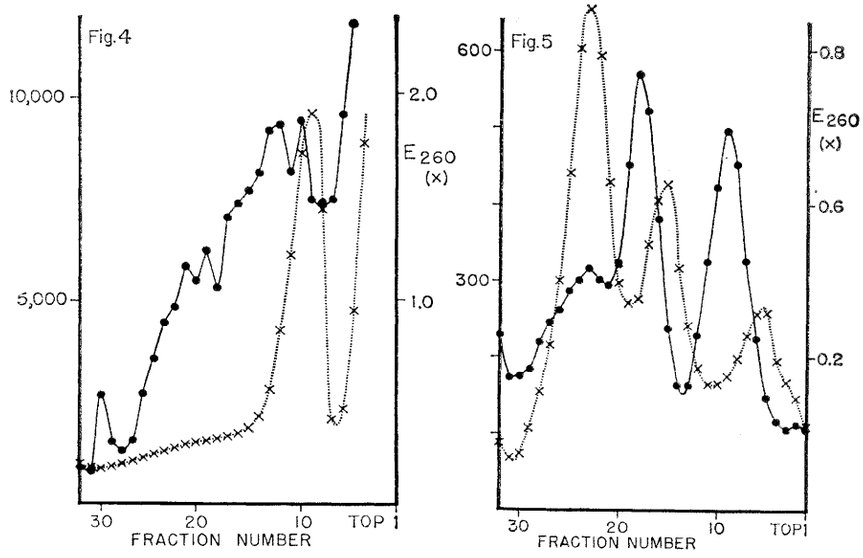

Fig. 4. Polyribosomes of cleavage-stage embryos. The 12,000*g* supernatant (*15*) of 6-hour embryos that had been incubated with 10 μM uridine-H^3 for 2 hours, from 4 to 6 hours after fertilization, was centrifuged through a 15 to 30 percent (by weight) sucrose gradient (*15*) for 2 hours in the Spinco SW 25.1 rotor at 24,000 rev/min. The location of labeled RNA was ascertained by precipitation of a portion of each fraction with cold 5 percent trichloroacetic acid and assaying the radioactivity of the precipitates (●).

Fig. 5. Sedimentation diagram of labeled RNA from polyribosomes of cleaving embryos. The region of the gradient of Fig. 4 containing polyribosomes labeled with uridine-H^3 (tubes 12 to 23) was shaken with an equal volume of phenol and the RNA of the aqueous phase was precipitated with ethanol. The sample of RNA was centrifuged through a sucrose gradient (5 to 20 percent) in the Spinco SW 39 rotor at 38,000 rev/min for 3.5 hours. ●, Incorporation of uridine-H^3; **X**, the absorbancy at 260 mμ.

but there was more associated with the region of the gradient heavier than that of the 28*S* ribosomal RNA component (Fig. 2) than elsewhere. A similar difference in distribution of the rapidly labeled RNA has been noted in early and late embryos of another species of sea urchin (*13*).

Cellular RNA may be partitioned by differential extraction. The aqueous phase of a simple phenol extraction yields the bulk of the cellular RNA, and, presumably, all of the cytoplasmic material. The residual gel interphase from this extraction contains most of the rapidly synthesized RNA and in some mammalian cells consists of nuclei (*3*); these nuclei have been designated here "phenolic nuclei." The sedimentation characteristics of the RNA obtained by a simple phenol extraction were compared with those of all the labeled RNA obtained by extraction with SDS-phenol at 60°C. After a pulse-labeling with uridine-H^3, 12-hour blastulae were homogenized in acetate buffer (*13*) without SDS and shaken with an equal volume of phenol at 20°C.

The gel interphase was saved for further analyses. The RNA of the aqueous phase was analyzed in the ultracentrifuge (Fig. 3*a*). The radioactivity was almost exclusively in the 4*S* component of the gradient. The radioactivity of the fraction other than 4*S* was too low to discern a meaningful sedimentation pattern. An equal portion of the same blastulae were extracted with SDS-phenol at 60°C. The radioactivity was greater, and essentially all of the additional material was in the region of the gradient heavier than 4*S* (Fig. 3*b*). A quantitative evaluation and the distribution of the radioactivity of the gel interphase can be obtained by subtracting the values of the curve of Fig. 3*a* from those of Fig. 3*b*. The result is that this pulse-labeled RNA is heavier than 4*S* and is polydisperse. This material represents essentially all of the rapidly labeled RNA (except 4*S*) of the cell, and, by analogy with other systems (*3*, *7*), also all of the rapidly labeled RNA of the nucleus.

The RNA of the "phenolic nuclei" from embryos at the four-cell and blastula stage was characterized for its ability to form hybrids with DNA prepared from sperm of the same species. The labeled RNA of the gel interphase was extracted with 0.5 percent SDS and phenol at 60°C. Hybridization (Table 1) was effected in the presence of unlabeled ribosomal and 4*S* RNA from unfertilized eggs or cleaving embryos. The stable components were obtained by extraction with phenol at 20°C, most of the nuclear RNA thus being excluded. Under these conditions a hybrid with labeled ribosomal and 4*S* RNA could not be detected. However, the pulse-labeled RNA easily formed hybrids, which were specific and resistant to ribonuclease (*14*). If the efficiency is 52 percent, calculated from various ratios of input RNA to DNA (Table 1), 77 and 65 percent respectively of this RNA is D-RNA. The remainder of the radioactivity, which may be attributed to precursors to ribosomal RNA (*7*), is small as compared to the large percentage of this component in later embryos (*13*) and in adult and tissue-culture cells (*7*). This synthesis of informational RNA takes place as early as the four-cell stage; the significance of such an early RNA synthesis needs clarification (*15*). The decrease with development in the percentage of D-RNA agrees with the relative rise in the rate of synthesis of ribosomal RNA, previously postulated (*13*) from studies similar to those of Figs. 1 and 2.

Cleavage-stage embryos were incubated with uridine-H^3 for 2 hours, homogenized, and then centrifuged to remove nuclei and mitochondria (*16*). The supernatant was placed on a sucrose gradient (*15*), and polyribosomes were detected by labeled RNA (Fig. 4). The region of the gradient containing polyribosomes was extracted directly with an equal volume of phenol. The labeled polyribosomal RNA was subjected to sedimentation analysis. This labeled RNA does not correspond to the optical density pattern of either ribosomal or 4*S* RNA (Fig. 5). However, the sedimentation pattern of optical density and labeled ribosomal and 4*S* RNA were coincident. The sedimentation constants (Fig. 5) were calculated (*16*) with the smaller, 18*S* ribosomal RNA as a reference. Highly resolved components of 10*S* and 22*S* were obtained, together with a peak at 28*S* and a shoulder, in this diagram, at 33*S*. Another component, at 38*S*, has been indicated in other analyses. All of these components were completely susceptible to the action of ribonuclease. Labeled DNA obtained by these and other procedures for extraction of RNA sedimented at 3*S*.

The newly synthesized polyribosomal RNA was examined for its ability to hybridize with DNA. RNA, labeled with uridine-H^3 and extracted directly from polyribosomes, was mixed with P^{32}-labeled ribosomal and 4*S* RNA, and equal samples of this mixture were placed on two sucrose gradients. The

Table 1. Hybrid formation between DNA and labeled RNA of sea-urchin embryos. Labeled RNA, dissolved in double strength SSC (= 0.15*M* NaCl plus 0.015*M* sodium citrate), was added to 56 μg of DNA, prepared from sperm of *Lytechinus pictus* (*20*), and the RNA : DNA ratio was adjusted to about 2 by the addition of unlabeled ribosomal and 4*S* RNA. Hybrid formation was allowed to occur in 0.5 ml of SSC for 24 hours and the hybrids were collected (*18*). Ribosomal and 4*S* RNA was obtained by extraction of gastrulae incubated with P^{32} overnight. (a) Non-4*S* RNA, pulse-labeled, was prepared from "phenolic nuclei." (b and c) The 2-hour embryos (4-cell stage) were incubated with 10 μM uridine-H^3 for a 10-minute pulse. (d) RNA from hybrid was the labeled RNA that was first combined with DNA entrapped in agar (*21*), then eluted from the agar and precipitated with ethanol. This RNA from the hybrid (purified D-RNA) was then used for hybrid formation again, the resulting percentage being taken as the efficiency of the method (*18*). This percentage would be in error to the extent that hybrid formation had some effect on its subsequent behavior of RNA. The values are averages of duplicate determinations. The values of radioactivity have been corrected for nonspecific binding of RNA to the membrane filters, which ranged from 0 to 5 percent of the input (*22*). For these amounts of input RNA, which were considerably below that necessary to saturate the DNA, the hybrids formed were found to be resistant to ribonuclease.

RNA				
Input		Unlabeled (μg)	Radioactive in hybrid (count/min)	Hybrid (%)
Activity (count/min)	Amount (μg)			
a. *Ribosomal + 4S RNA*				
800	5.0	0	2	0.3
1600	10.0	116	6	0.4
b. *Non-4S RNA, pulse-labeled, 4-cell cleavage*				
1052	4.6	116	422	40.1
1884	8.2	116	745	39.5
c. *Non-4S RNA, pulse-labeled, blastula (12-hr)*				
680	3.0	56	233	34.3
1359	6.0	56	448	33.0
2039	9.0	56	751	36.8
2718	12.0	56	950	35.0
d. *RNA from hybrid (purified D-RNA)*				
166	15.0	0	87	52.4
219	1.5	116	114	52.0
657	4.5	116	334	50.8

gradients were centrifuged at the same time, and equal numbers of fractions collected from each. The fractions of one gradient were assayed for radioactivity directly (*17*). The fractions from the other gradient were collected in another series of vials, to which unlabeled ribosomal and 4*S* RNA and DNA were added. Hybrid formation was allowed to occur, and the solutions were passed through membrane filters which retained DNA-RNA hybrids (*18*, *20*). The radioactivity on the membrane filters was assayed in a liquid (toluene) scintillation counter (Fig. 6). The incorporations of the H^3-labeled polyribosomal RNA and the P^{32}-labeled ribosomal and 4*S* RNA of the first gradient were the inputs for the hybrid formation of each gradient fraction. The P^{32} served both as marker for the sedimentation positions of the ribosomal and 4*S* RNA and as an internal control, to ascertain the extent of DNA-RNA hybrid formation. Thus hybrids with ribosomal and 4*S* RNA were again not detectable. However, a substantial amount of the labeled polyribosomal RNA formed a hybrid; the average of all the points in Fig. 6 was 33 percent. Therefore, from the efficiency of this method (Table 1), we can account for about 63 percent of this RNA as D-RNA. The distribution of the hybrid, thus that of the D-RNA, is exactly that of the discrete sedimenting classes of the polyribosomal RNA.

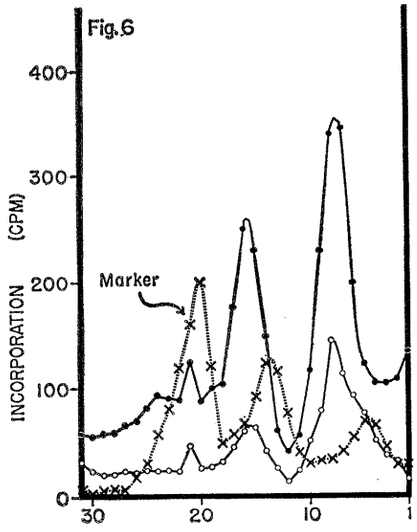

Fig. 6. Sedimentation diagram of D-RNA of polyribosomes. Two parallel gradients are compared. Incorporation of uridine-H^3 (●) in the RNA of polyribosomes and of P^{32} (X) in marker ribosomal and 4*S* RNA are plotted with the incorporation of uridine-H^3 in the DNA-RNA hybrids (O) formed from each corresponding fraction (Table 1).

The sedimentation behavior of labeled RNA derived from the polyribosomes of later-stage embryos indicates that (i) there was considerable synthesis of ribosomal RNA and (ii) the polyribosomes actively synthesizing protein corresponded to those containing newly synthesized RNA, unlike the early-stage embryo in which the most active polyribosomes contained the least amount of new RNA (*15*). The newly synthesized RNA of the active polyribosomes of the 44-hour pluteus was extracted and the same sedimentation classes were noted as in the early stages represented by Figs. 5 and 6. Some 4*S* RNA is present as well (Fig. 7*a*). Thus these peculiar sedimentation properties are presumably not related to developmental stage or to the condition of activity or inactivity of the polyribosomes. The sedimentation diagram of the RNA of the ribosomal component in the same gradient from which the polyribosomes of the pluteus were obtained serves as a control in that it shows the 28*S* and 18*S* ribosomal RNA's together with a predominant 4*S* component (Fig. 7*b*).

The sedimentation patterns of the total pulse-labeled RNA of cleaving embryos and blastulae were not distinctive (*4*, *7*, *11*, *12*). However, the mRNA of the polyribosomes displayed a pattern of discrete sedimenting components. The distribution of mRNA (so designated by virtue of its polyribosomal origin and DNA-like character) in what may be regarded as discrete size classes suggests that either (i) mRNA is transcribed in discrete sizes, (ii) the emergence of discrete sizes occurs after transcription, or (iii) the discrete sedimenting components are in themselves complexes with ribosomal RNA. The first possibility cannot easily be reconciled with the apparent size continuum of the rapidly synthesized nuclear RNA, unless this continuum is due partly to the extraction of unfinished or nascent RNA, and perhaps to sedimentation artifacts. The skewed distribution of rapidly synthesized RNA toward the very heavy region of the gradient (Fig. 2) is even more pronounced in sedimentation diagrams obtained with other biological material (*7*), often revealing a predominant 45*S* component. Since this component has been implicated as precursor to 28*S* and 18*S* ribosomal RNA (*7*), a transformation subsequent to transcription is also inferred. Thus such a transformation may be similarly operative, in accord with our second alternative, for the formation of discrete sizes of mRNA. The last explanation (iii) involving complexes with ribosomal RNA is unlikely, since we

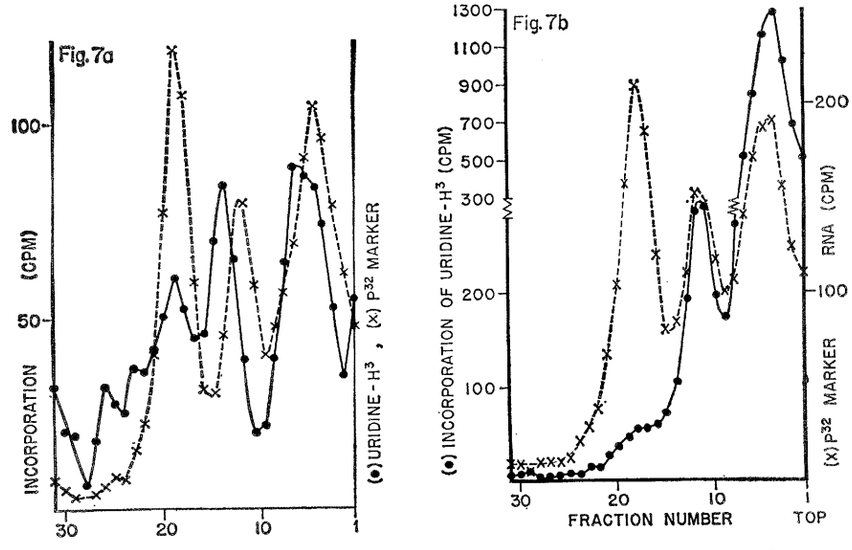

Fig. 7. Sedimentation diagrams of labeled RNA from polyribosomes and ribosomes of the 44-hour pluteus. Embryos (1 ml per 5 ml of sea water) were incubated in 5 μM uridine-H^3 for 60 minutes (from 44 to 45 hours after fertilization). RNA was extracted and analyzed as in Fig. 5. (*a*) RNA from polyribosomes. (*b*). RNA from ribosomes. ●, Uridine incorporation; X, P^{32} marker.

have been able to isolate similar discrete sedimenting classes of RNA from mRNA-protein particles (*14*, *19*) which are widely separated from ribosomes and polyribosomes on sucrose gradients. The size of the RNA appears to depend only on the size of the mRNA-protein particle from which it was derived. Thus a 57*S* particle contains only 33*S* RNA and a 21*S* particle contains only 11*S* RNA. Such a distribution of classes of RNA in these particles lends credence to the existence of disrete size classes of messenger RNA in the polyribosomes.

MARTIN NEMER
ANTHONY A. INFANTE
Institute for Cancer Research, Fox Chase, Philadelphia 11, Pennsylvania

References and Notes

1. F. Jacob and J. Monod, *J. Mol. Biol.* **3**, 318 (1963); F. Gros, H. Hiatt, W. Gilbert, C. G. Kurland, R. W. Risebrough, J. D. Watson, *Nature* **190**, 581 (1961).
2. T. R. Warner, P. M. Knopf, A. Rich, *Proc. Natl. Acad. Sci. U.S.* **49**, 122 (1963); F. O. Wettstein, T. Staehlin, H. Noll, *Nature* **197**, 430 (1963); A. Gierer, *J. Mol. Biol.* **6**, 148 (1963).
3. A. Sibatani, S. R. deKloet, V. G. Allfrey, A. E. Mirsky, *Proc. Natl. Acad. Sci. U.S.* **48**, 471 (1962); G. P. Georgiev and V. L. Mantieva, *Biochim. Biophys. Acta* **61**, 153 (1962).
4. H. H. Hiatt, *J. Mol. Biol.* **5**, 217 (1962).
5. B. H. Hoyer, B. J. McCarthy, E. T. Bolton, *Science* **140**, 1408 (1963).
6. G. Brawerman, L. Gold, T. Eisenstadt, *Proc. Natl. Acad. Sci. U.S.* **50**, 630 (1963).
7. R. P. Perry, *ibid.* **48**, 2179 (1962); ———, P. R. Srinivasan, D. E. Kelley, *Science* **145**, 504 (1964); K. Scherrer, H. Latham, T. E. Darnell, *Proc. Natl. Acad. Sci. U.S.* **49**, 240 (1963).
8. J. E. M. Midgeley and B. T. McCarthy, *Biochim. Biophys. Acta* **61**, 696 (1962).
9. S. Penman, K. Scherrer, Y. Becker, T. E. Darnell, *Proc. Natl. Acad. Sci. U.S.* **49**, 654 (1963).
10. A. C. Trakatellis, A. E. Axelrod, M. Montjar, *J. Biol. Chem.* **239**, 4237 (1964).
11. K. Scherrer and T. E. Darnell, *Biochem. Biophys. Res. Commun.* **7**, 486 (1962).
12. M. Hayashi and S. Spiegelman, *Proc. Natl. Acad. Sci. U.S.* **47**, 1564 (1961).
13. M. Nemer, *ibid.* **50**, 230 (1963).
14. ——— and A. Infante, in preparation.
15. A. S. Spirin and M. Nemer, *Science*, this issue.
16. R. G. Martin and B. N. Ames, *J. Biol. Chem.* **236**, 1372 (1961).
17. G. A. Bray, *Anal. Biochem.* **1**, 279 (1960).
18. A. P. Nygaard and B. D. Hall, *Biochem. Biophys. Res. Commun.* **12**, 98 (1963); E. H. McConkey and T. W. Hopkins, *Proc. Natl. Acad. Sci. U.S.* **51**, 1197 (1964).
19. M. Nemer and A. A. Infante, *Federation Proc.* **24**, 283 (1965).
20. E. H. Szybalska and W. Szybalska, *Proc. Natl. Acad. Sci. U.S.* **48**, 2026 (1962).
21. E. T. Bolton and B. J. McCarthy, *ibid.*, p. 1390.
22. The controls used to determine nonspecific binding of RNA to the membrane filters were: (i) DNA was added to the RNA immediately before filtration, (ii) RNA and DNA were incubated separately at 60° or 0°C for 24 hours and then mixed immediately before filtration, and (iii) RNA and DNA were maintained together at 0°C for 24 hours.
23. Supported by grants CA 05936-04 and CA 06927-03 from the National Institutes of Health.

29 March 1965

Bone Density Measurements in vivo: Improvement of X-ray Densitometry

Abstract. *An X-ray bone densitometer has been developed which makes direct tracings of absorption curves on a nearly linear scale. Speed and precision are increased by elimination of x-ray film. Results are reproducible to within 3 percent with a phantom finger, and within 6 percent with human subjects.*

Research to improve methods of measuring bone density in vivo continues (*1*). Our laboratory, which uses the left phalanx 5-2 for measurements, has developed an x-ray bone densitometer (*2*) to increase speed and precision in bone density determinations. Greater precision is attained by the elimination of x-ray film with its error, and by the reduction of scatter through collimation. The densitometer uses a low-intensity x-ray beam as the source of energy and utilizes a scintillation detector conjoined with a photomultiplier tube. It incorporates an electronic circuit which utilizes the logarithmic characteristic of the photomultiplier tube to produce linear absorption curves directly on graph paper by an *x-y* recorder. Figure 1 shows a block diagram of the bone densitometer. Not only is x-ray film eliminated from the procedure but approximate linearity is achieved for the absorption curves of the reference standard and test object. The instrument was calibrated at the factory with the same alloy standard used in this laboratory in the film method of bone density measurement (*3*). Daily calibrations are made with a secondary standard.

The collimated x-ray beam is located near the finger to reduce scatter and exposure to the subject. The effective radiation received at the operational setting of 40 kv and 5 ma is about 500 mr per trace. This dose is considered minimal, since it is to a narrow path of a body extremity. The x-ray tube is so shielded that radiation is negligible in the vicinity of the instrument, including operator and subject positions. The bone densitometer has an adjustable stand designed for scanning the left phalanx 5-2. The absorption curve for the chosen pathway is traced directly as the stand carries the finger through the x-ray beam. The slit size of the beam is 1 by 3 mm. The stand travels through the x-ray beam at the rate of 1 inch (2.5 cm) per 56 seconds. There are two hand positions, so that antero-posterior and lateral scans can be made. With these two scans to furnish linear measurements, the cross-sectional areas of bone and flesh used in the calculation of the bone density index are determined as ellipses with two measured axes. Figure 2 shows absorption curves of a central pathway of phalanx 5-2 as traced directly by the bone densitometer.

The bone densitometer is portable and is designed to fit into a station wagon. It operates from a 115-volt, 60-cy standard electrical outlet.

Machine reproducibility was deter-

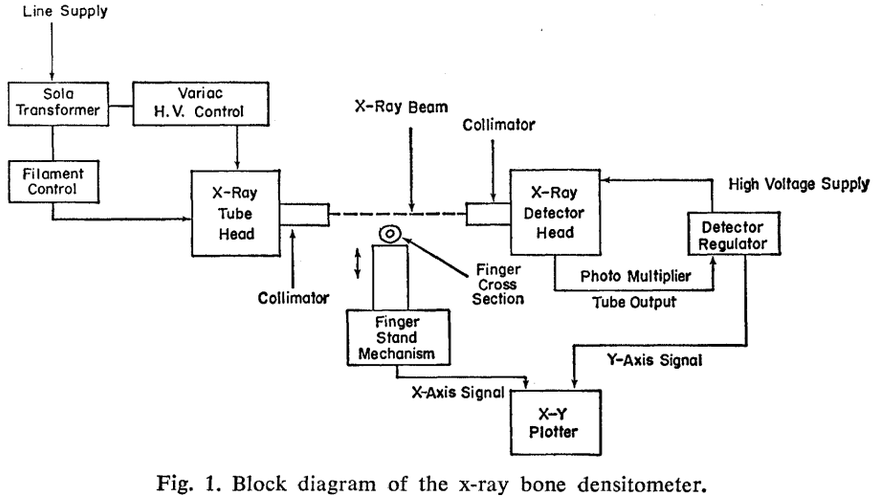

Fig. 1. Block diagram of the x-ray bone densitometer.